Applied Energy 305 (2022) 117962

Contents lists available at ScienceDirect

Applied Energy

journal homepage: www.elsevier.com/locate/apenergy

Accurate and reliable state of charge estimation of lithium ion batteries using time-delayed recurrent neural networks through the identification of overexcited neurons

Zhimin Xi [a,*], Rui Wang [a], Yuhong Fu [b], Chris Mi [b]

[a] Department of Industrial and Systems Engineering, Rutgers, The State University of New Jersey, 96 Frelinghuysen Road, Piscataway, NJ 08854, United States
[b] Department of Electrical and Computer Engineering, San Diego State University, 5500 Campanile Drive, San Diego, CA 92130, United States

HIGHLIGHTS

- Time-delayed recurrent neural network (TD-RNN) was proposed for lithium ion battery SOC estimation.
- Neurons states were checked through time frequency analysis for identifying 'overexcited' neurons.
- Expectational battery SOC estimation accuracy is consistently obtained using the TD-RNN without 'overexcited' neurons.

ARTICLE INFO

Keywords:
Lithium ion battery
State of charge
Time-delayed recurrent neural network
Overexcited neurons
Equivalent circuit models

ABSTRACT

Various neural network models have been adopted for lithium ion battery state of charge (SOC) estimation with good accuracy. However, problems for battery states estimation from neural networks were usually not reported, which is mainly due to the lack of effective solutions other than a trial and error training process. This paper firstly proposes time-delayed recurrent neural network for lithium ion battery modeling and SOC estimation. Both exceptional performances and unexpected overfitting or poor performances are reported with in-depth analysis of the root cause. With explicit formulation of the network, each hidden neuron's output is examined. It is discovered that overexcited neurons could be the root cause for unexpected poor performances of the neural network. Without overexcited neurons, expectational SOC estimation accuracy is consistently obtained with estimation error being less than 1% for lithium ion magnesium phosphate ($LiFeMgPO_4$) batteries considering a fair comparison in literature.

1. Introduction

Accurate estimation of lithium ion battery state of charge (SOC) is important since it tells the user the amount of 'fuel' left for the systems or devices powered by the battery such as electrified vehicles, unmanned aerial vehicles, and cell phones. The fact that there are so many papers studying battery SOC estimation is because of the technical difficulty for an accurate estimation under arbitrary battery operating conditions for different types of lithium ion batteries.

Battery models can be classified into three major groups as electrochemical models [1–5], equivalent circuit models [6–10], and machine learning models [11–17]. Electrochemical models are generally considered as computationally expensive and hence are not suitable for battery SOC estimation in real-time. Even though various reduced-order models were developed through simplifications and assumptions, the SOC estimation accuracy is similar to the equivalent circuit model [18]. There are a variety of battery equivalent circuit models where circuit components such as resistance and capacitance are used to approximate the dynamics of the battery [6]. These models are computationally efficient with a reasonably good accuracy for most lithium ion batteries. However, most models rely on an open circuit voltage (OCV) vs. SOC curve to build functional relationship between the hidden state (i.e., SOC) and directly measurable quantity such as battery current and terminal voltage. When such an OCV-SOC curve contains a relatively flat region such as in lithium ion magnesium phosphate ($LiFeMgPO_4$) batteries, SOC estimation was not as accurate as other types of lithium ion batteries [16]. Besides, the model parameters usually vary at different battery SOC and aging levels, which make accurate SOC estimation

* Corresponding author.
E-mail address: zhimin.xi@rutgers.edu (Z. Xi).

https://doi.org/10.1016/j.apenergy.2021.117962
Received 22 March 2021; Received in revised form 24 September 2021; Accepted 27 September 2021
0306-2619/Published by Elsevier Ltd.

more difficult during its life cycle. In practice, the equivalent circuit models are usually applied together with different filtering algorithms (e.g., Kalman filters and particle filters) [19–21] for battery SOC estimation under dynamic charging/discharging profiles.

Machine learning models are recently gaining popularity for battery SOC estimation. Typical models include Gaussian process, feedforward neural network, time-delayed neural network, recurrent neural network (RNN), and long short-term memory (LSTM) neural network. The major limitation of various neural network models is being a black box. With random weight initialization, converged training results at different local optimums could result in different performances for batteries under new operating conditions. Furthermore, it is difficult to identify the root cause and explain the results. Nevertheless, accurate results for SOC estimation were reported using different machine learning methods. Kang et al. [11] employed radial basis function neural network for SOC estimation of lithium ion manganese oxide ($LiMn_2O_4$) batteries considering the aging effect. SOC estimation error was reported within 5% or less. Chaoui et al. [12] used time-delayed neural network to estimate both battery SOC and state of health for lithium ion phosphate ($LiFePO_4$) batteries. However, the SOC estimation accuracy was only reported under constant charging and discharging current profiles. Xia et al. [13] proposed wavelet neural network by replacing the linear output layer as a wavelet function and applied the model for SOC estimation of Samsung ICR-18650-22P ($LiNiMnCoO_2$) batteries. SOC estimation error was reported within 5% under different current profiles. Chemali et al. [14] reported a low SOC mean absolute error of 0.573% at a fixed ambient temperature condition with proper training for Panasonic 18650PF ($LiNiCoAlO_2$) batteries using the LSTM neural network. Yang et al. [15] employed the LSTM for SOC estimation of A123 18,650 batteries ($LiFePO_4$) where the SOC estimation error was generally below 5% but with sudden error increase and some noisy behaviors. In addition, the performance did not show dominant advantages compared to an unscented Kalman filter approach with an equivalent circuit model. Xi et al. [16] employed Gaussian process for learning of model bias from equivalent circuit models, and then used the corrected model to estimate SOC for lithium-ion magnesium phosphate ($LiFeMgPO_4$) batteries. Due to the flatness of the OCV-SOV curve, the typical equivalent circuit models can only reach less than 10% estimation error, but the error was reduced to be less than 5% with the aid of the Gaussian process for bias correction. Hong et al. [17] employed the LSTM neural network for battery SOC estimation considering weather parameters. To prevent overfitting, the dropout technique [22] was employed. They reported within 2% SOC estimation error for the studied battery. However, battery type information was not provided.

There are a few common limitations of existing work by employing various neural network models for battery SOC estimation. Firstly, they were mainly applying existing network structures for battery SOC estimation. Secondly, the performances from the neural network models were not often compared with equivalent circuit models. From limited reported results, they do not perform dominantly better than the equivalent circuit models [15]. Thirdly, problems of the neural network models for battery SOC estimation were usually not studied or reported. Poor performances are often attributed to inappropriate training processes. The common solutions are usually to retrain the network with more or less layers, neurons, and adding a dropout layer with certain dropout probability to prevent overfitting. Such an overall trial and error process makes neural network models less attractive for battery states estimation especially when the results are also difficult to explain.

Contribution of this paper is three-fold. Firstly, we propose time-delayed RNN (TD-RNN) for lithium ion battery SOC estimation, which should be a more suitable network structure for lithium ion battery states estimation. Secondly, we analyze exceptional and poor performances of the battery SOC estimation results from the proposed TD-RNN and further identify the possible root cause. Thirdly, we compare the results to the study using equivalent circuit models and the LSTM neural network. The studied battery is lithium ion magnesium phosphate ($LiFeMgPO_4$) battery, which has a relatively flat OCV-SOC curve that makes accurate SOC estimation difficult.

The rest of the paper is organized as follows. Section II elaborates data generation including simulation and experiment data. Section III presents the proposed TD-RNN modeling and formulation for battery terminal voltage prediction and qualitatively analyzes its modeling similarity with the equivalent circuit model. Section IV presents exceptional and unexpected overfitting performances of the TD-RNN using both simulation and experimental data, and analyzes the root cause through examining the output from each neuron. Section V proposes time frequency analysis to quantitatively identify the 'overexcited' neurons so that exceptional performance of the TD-RNN can be maintained while avoiding unexpected poor performances. Section VI further discusses the robustness of the TD-RNN and provides comparison study with the LSTM neural network and the equivalent circuit model. Finally, conclusion and future work are presented in Section VII.

2. Data generation – Simulation and experimental data

Both simulation and experimental data were obtained using Valence 26,250 lithium-ion magnesium phosphate ($LiFeMgPO_4$) batteries with a 2.5 Ah nominal capacity. Simulation data were generated based on a first-order resistance–capacitance (RC) battery model formulated as

$$\begin{cases} x_k = x_{k-1} - \Delta t i_k / C_r \\ z_k = OCV(x_k) + i_k R(x_k) + U_{1,k} \\ U_{1,k} = exp(-\Delta t/\tau_1(x_k))U_{1,k-1} + R_1(x_k)[1 - exp(-\Delta t/\tau_1(x_k))]i_k \end{cases} \quad (1)$$

where x_k, i_k, z_k are battery SOC, current, and terminal voltage at time step k, respectively; Δt is the discrete time interval; C_r is the rated battery capacity; $OCV(x_k)$ is a nonlinear function of battery open circuit voltage at given SOC values, i.e., the OCV-SOC curve; $R(x_k)$ is battery charging/discharging resistance as a nonlinear function of battery SOC; $U_{1,k}$ is a recursive term due to the RC pair; $\tau_1(x_k)$ and $R_1(x_k)$ are time constant and resistance of the first RC pair, respectively, and both are nonlinear functions of battery SOC. Battery OCV-SOC curve and parameters were obtained through battery characterization tests and results were reported in the authors' previous work [16]. Hence, simulation data of the terminal voltage were obtained using the battery model in Eq. (1) given any current profile with the known initial SOC value. For experimental data, actual measured terminal voltage data were obtained under three current profiles including the urban dynamometer driving schedule (UDDS), the New York city cycle (NYCC), and the mixture of the two cycles (i.e., one UDDS cycle followed by one NYCC cycle as a complete cycle denoted by UDDS-NYCC). In particular, the cycle currents were scaled such that the maximum current was at a 5C rate. The initial SOC was configured at 90% and the cycles were repeated till the SOC reached 20%. The experiments were conducted at room temperature.

3. TD-RNNS for battery modelling

For terminal voltage modeling using the TD-RNN, battery SOC and current can be represented as an input vector with $x_{i,k}$ indicating the i^{th} input parameter at time step k. For the simplest TD-RNN with only one hidden neuron and one time-delay step as shown in Fig. 1a, the functional output at each layer (i.e., input layer, hidden layer, and output layer) is provided at the right-hand side of the figure. The same parameter notations are used at different layers in order to reduce the notation complexity when extending it to a more complex network structure. The input to one hidden neuron at the k^{th} time step (i.e., $Z_{1,k}$) includes the weighted sum of each input node, the weighted recurrent output of the hidden neuron at previous time step (i.e., $y_{1,k-1}$), and a bias term of the hidden neuron (i.e., b_1). The output of the hidden neuron at the k^{th} time step $y_{1,k}$ is determined by a transfer (or activation) function $f(\bullet)$ which takes the input $Z_{1,k}$. Finally, the output layer node computes the terminal voltage based on a linear function, i.e., the weighted $y_{1,k}$ with an addition of the bias term of the output layer node. Typically, all

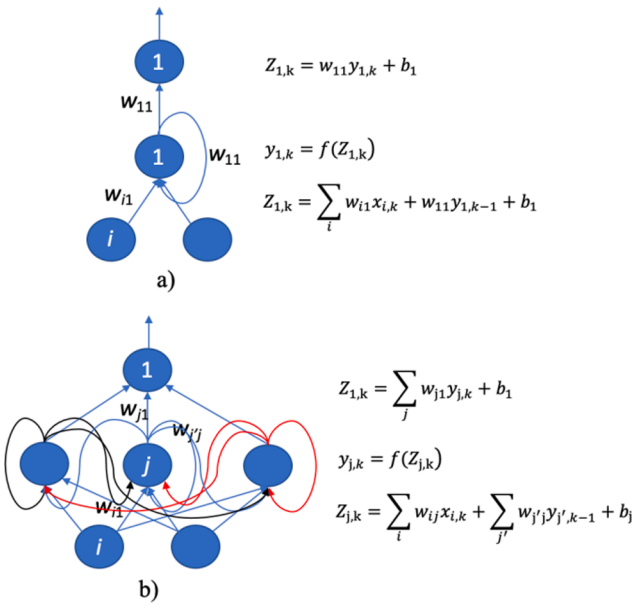

Fig. 1. Schematic diagram and functional formulations of TD-RNNs with one time-delay step.

input and output nodes are normalized during the training stage and the output should be denormalized for prediction. The number of parameters that needs to be optimized is 6 for this simplest structure. With a hyperbolic tangent sigmoid transfer function, formulation in Fig. 1a can be rewritten as

$$\begin{cases} Z_{1,k} = w^o_{11}y_{1,k} + b^o_1 \\ y_{1,k} = 2/\left\{1 + exp\left[-2\left(\sum_i w^i_{i1}x_{i,k} + w^r_{11}y_{1,k-1} + b^h_1\right)\right]\right\} \end{cases} \quad (2)$$

where upper scripts of the parameter, i.e., *o*, *i*, *r*, and *h*, are added to distinguish the parameter difference at output, input, recurrent, and hidden layer, respectively. By comparing with the first-order RC model in Eq. (1), similarity of the two equations can be observed such as sharing a recursive function term. In particular, the battery model parameters in Eq. (1) are dependent on its SOC state. As such, we can think of a large set of model parameters in Eq. (1) whereas Eq. (2) contains only 6 parameters.

Using the battery model parameters and characteristics determined through the offline test, battery terminal voltage under the UDDS profile can be determined based on Eq. (1) with an initial SOC set as 90%. To test the modeling capability of the TD-RNN with only one hidden node, the network was trained using time-series SOC and current as inputs, and the corresponding terminal voltage as the outputs. The terminal voltage comparison results are shown in Fig. 2a where the first-order RC model prediction was treated as the true result. In particular, the output from the hidden node (i.e., $y_{1,k}$) was also presented in Fig. 2a since this is the main nonlinear component of the network. It can be observed that the overall training results are satisfactory with only one hidden neuron. As shown in Fig. 2b, the voltage calibration error could reach about 100 mV, which is considerably large for battery voltage and SOC estimation. A desired error magnitude should be less than 10 mV in order to maintain accurate SOC estimation for this type of lithium ion battery. In addition, the neuron output takes the main responsibility for capturing the nonlinear behavior of the terminal voltage.

When more neurons are used in the TD-RNN, Fig. 1b shows the extension and its formulation where index i indicates the i^{th} input parameter, and index j represents the j^{th} hidden neuron. The number of network parameters increases significantly especially for the weight parameter of the fully connected recurrent part. For example, for the network with 5 hidden neurons, the total number of network parameter is: $2 \times 5 + 5 \times 5 + 5 + 5 + 1 = 46$. A further extension is to include more time-delay steps such as $y_{j',k-2}$ and $y_{j',k-3}$ with their own weight parameters. As such, for n time-delay steps, the total number of network parameter is: $2 \times 5 + 5 \times 5 \times n + 5 + 5 + 1$. A more general formulation for TD-RNN can thus be written as

$$\begin{cases} Z_{1,k} = \sum_j w^o_{j1}y_{j,k} + b^o_1 \\ y_{j,k} = 2/\left\{1 + exp\left[-2\left(\sum_i w^i_{ij}x_{i,k} + \sum_m \sum_{j'} w^{r,m}_{j'j}y_{j',k-m} + b^h_j\right)\right]\right\} \end{cases} \quad (3)$$

where m (=1, 2, …, M) is the index for the number of time-delay steps, j' is the dummy index of j; $w^{r,m}_{j'j}$ is the weight of the recurrent layer from the j'^{th} neuron to the j^{th} neuron at the corresponding time-delay step m. By revisiting Fig. 1b, it is clear that each hidden neuron is in charge of learning part of the nonlinearity of the system input–output relationship with information from other neurons at previous time steps. The final output is just a simple linear combination of each hidden neuron's output. Hence, to better understand the performance of the TD-RNN for lithium ion battery voltage and SOC estimation, it is necessary to dive deeper to check each hidden neuron's output.

Similar to the battery voltage calibration using the simulation data from the first-order RC model, TD-RNNs with two and five hidden neurons were employed for the voltage calibration, and the output from each neuron is shown in Fig. 3a and c, respectively. Firstly, the expected result is that voltage calibration error has been significantly reduced as shown in Fig. 3b and 3d. In particular, the error is less than 4 mV most of

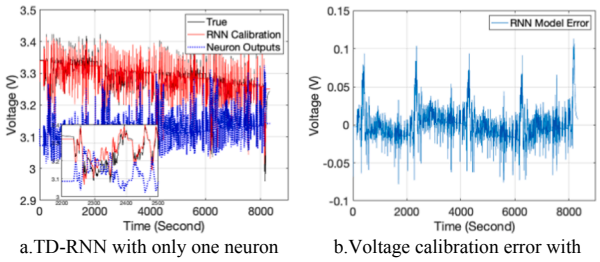

a.TD-RNN with only one neuron b.Voltage calibration error with only one hidden neuron

Fig. 2. Performance of terminal voltage calibration of the TD-RNN with only one hidden neuron.

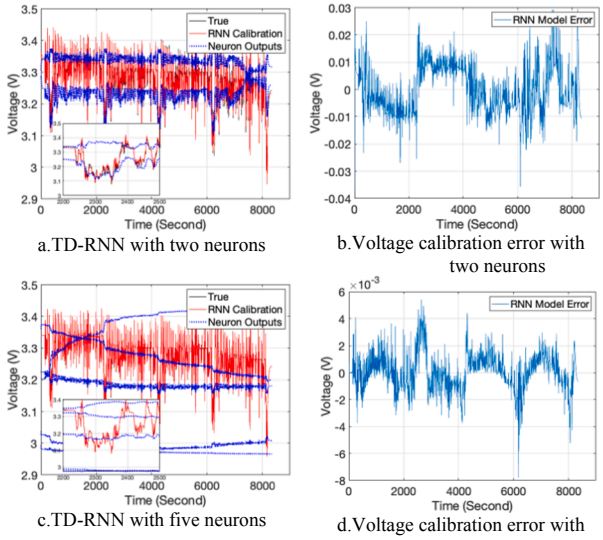

a.TD-RNN with two neurons b.Voltage calibration error with two neurons

c.TD-RNN with five neurons d.Voltage calibration error with five neurons

Fig. 3. Performance of terminal voltage calibration of TD-RNN with two and five hidden neurons.

the time with five hidden neurons. Secondly, with more hidden neurons to share the task of approximating the nonlinear battery model, each neuron's output seems to be more stable without abrupt changes within the short period of time as observed in Fig. 3a and c.

4. Performances of TD-RNN with and without overexcited neurons

To demonstrate the practical usefulness of machine learning models including the TD-RNN, the model should be able to predict battery performances accurately under new battery operating conditions. This section demonstrates the performance using both simulation data generated from the first-order RC model and the experimental data.

4.1. Simulation data

Using the first-order RC model as a reference to generate battery terminal voltage data given the true battery SOC and current profiles, performance of the TD-RNN can be verified through simulation study. The reason of using simulation data is to demonstrate the modeling capability of the TD-RNN for a known nonlinear battery model, thus to better understand the network configuration with respect to its modeling capability. In this study, terminal voltage under the UDDS current profile was used as training data sets for a defined TD-RNN with seven hidden neurons and one time-delay step. After the training, the TD-RNN was used to predict terminal voltage of the battery under two new current profiles, i.e., the UDDS-NYCC and the NYCC profile, and the predictions were compared to the true value. Fig. 4a and b show the accuracy of the voltage calibration, where the voltage calibration error is less than 2 mV most of the time. In particular, seven neuron outputs as shown in Fig. 4a are relatively stable. According to the rationale described above based on the observation in Fig. 3, each neuron is sharing the load to approximate the nonlinear battery function. Consequently, voltage predictions of the TD-RNN for two other current profiles are accurate as shown in Fig. 4c – f. Particularly, NYCC is a quite different current profile compared to the UDDS, and yet the voltage prediction error is less than 4 mV most of the time. This example clearly demonstrates the exceptional performance of the TD-RNN for approximating the first-order RC model.

On the other hand, unexpected overfitting could occur for the TD-RNN, which is not directly observable through the typical voltage calibration process. Fig. 5a and b show the voltage calibration error of the TD-RNN under UDDS current profile when two time-delay steps were used. The voltage calibration error is again mostly less than 2 mV. However, the neuron outputs shown in Fig. 5a are quite noisy or 'overexcited'. When this trained TD-RNN was applied to two other battery current profiles for predicting the terminal voltage, unexpected voltage overfitting occurs as shown in Fig. 5c-f. This phenomenon can be repeatedly observed indicating that the 'overexcited' neurons are related to the overfitting of the TD-RNN.

Another important finding through the simulation data is related to the reason of having 'overexcited' neurons. As the first order RC model contains only one recursive term, the TD-RNN with two time-delay steps would essentially make the model too complex to fit the first order RC model. Consequently, 'overexcited' neurons are often observed.

4.2. Experimental data

Accurate SOC estimation of this type of lithium ion battery is challenging using various battery equivalent circuit models (e.g., first-order RC and second-order RC models) even with advanced bias learning

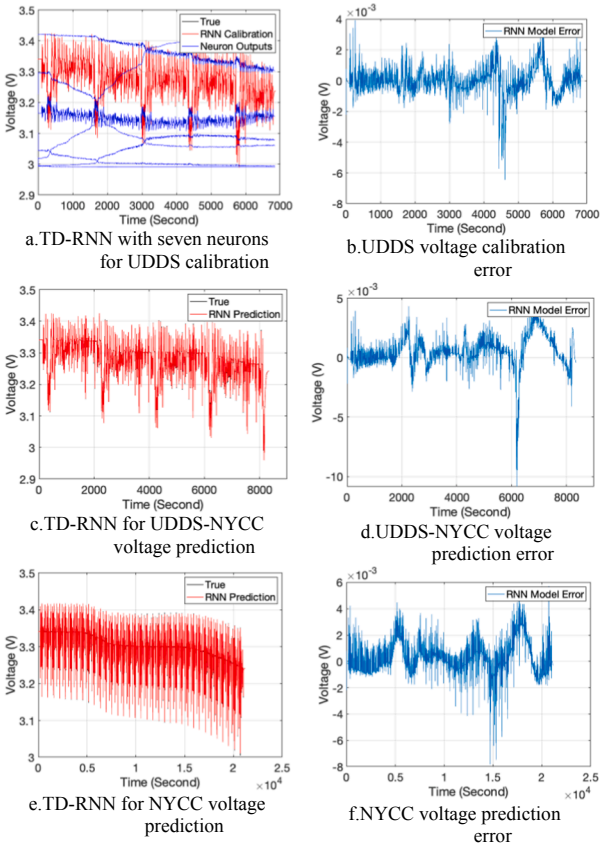

Fig. 4. TD-RNN with exceptional performance using one time-delay step and seven hidden neurons for battery voltage calibration and prediction under UDDS (a and b), UDDS-NYCC (c and d), and NYCC (e and f) profiles.

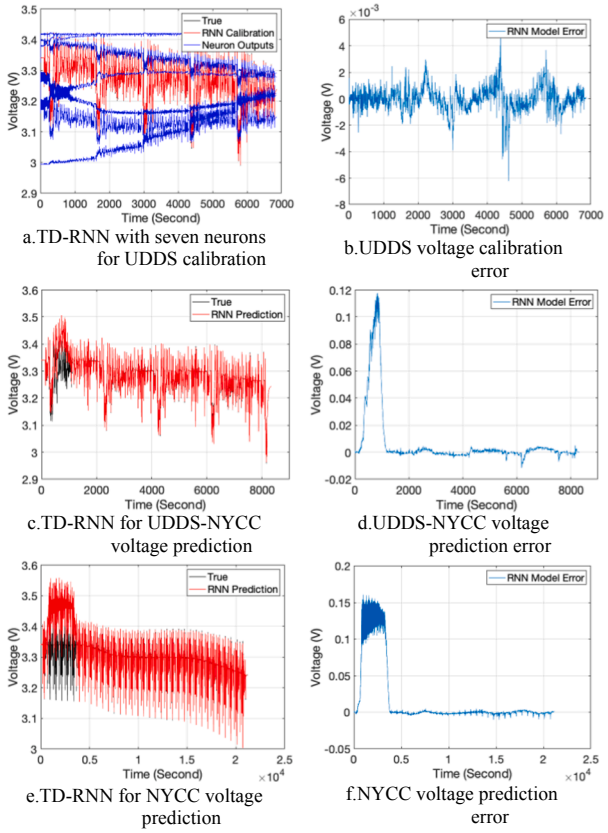

Fig. 5. TD-RNN with unexpected over-fitting using two time-delay steps and seven hidden neurons for battery voltage calibration and prediction under UDDS (a and b), UDDS-NYCC (c and d), and NYCC (e and f) profiles.

methods as reported in [16]. The best results achieved were to obtain about 5% SOC estimation errors on average. In this study, the UDDS-NYCC profile was firstly employed to train a TD-RNN with five time-delay steps and seven hidden neurons, then the model was used to estimate battery SOC under UDDS and NYCC profiles. Fig. 6 shows one exceptional performance of the model where the SOC estimation error is consistently below 1% for two test profiles as shown in Fig. 6c-f. In particular, seven neuron outputs in Fig. 6a are quite stable.

Unlike the filtering based SOC estimation methods, initial guess of the SOC is not needed using the TD-RNN. Battery SOC is directly predicted based on the time series data from the voltage and current. To further demonstrate the robustness of the method, partial test data from UDDS and NYCC profiles were used to predict the SOC. In particular, initial SOCs were set at 76% and 61% as shown in Fig. 7 and Fig. 8, respectively. A few findings are observed based on the results. Firstly, the initial SOC prediction from the TD-RNN seems to relate to the training data which starts at 90% SOC as shown in Fig. 6a. Secondly, SOC prediction accuracy is not as good as shown in Fig. 6c-f, which indicates that different initial conditions between training and testing influence the prediction accuracy. Thirdly, further change of the initial SOC as compared in Fig. 7 and Fig. 8 does not influence the model prediction capability, which is a desired property to make the model practically useful.

It should be noted that the training process for the TD-RNN contains randomness due to the random weight initialization. As such, the training results could be different with the same network structure. Fig. 9a and b present the training results with the same network structure as in Fig. 6. Although the calibrated SOC matches the true SOC very well, some of the neuron outputs are quite noisy during some time periods. When this TD-RNN was used for estimation of the battery SOC under two new current profiles, large SOC estimation errors were observed as shown in Fig. 9c-f. It is difficult to explain the unstable

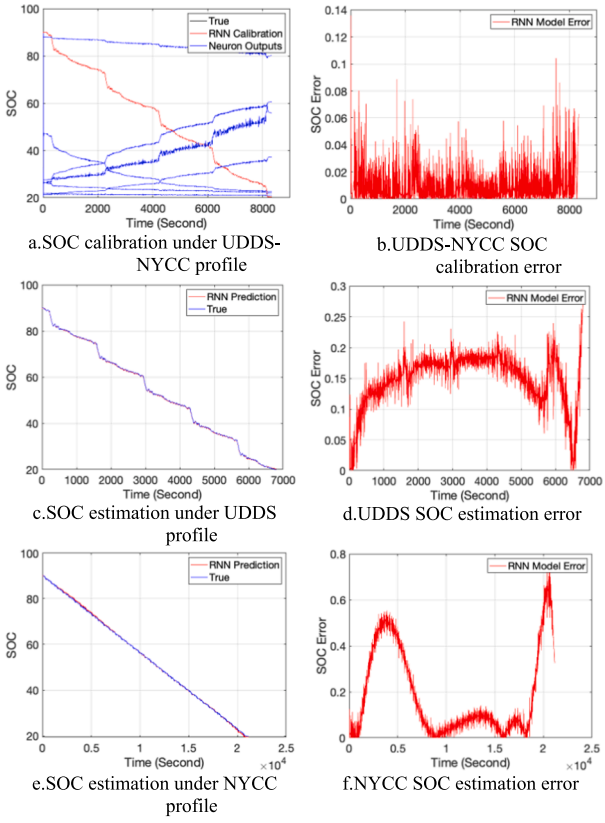

Fig. 6. TD-RNN without overexcited neurons using five time-delay steps and seven hidden neurons for battery SOC calibration and prediction under UDDS-NYCC (a and b), UDDS (c and d), and NYCC (e and f) profiles.

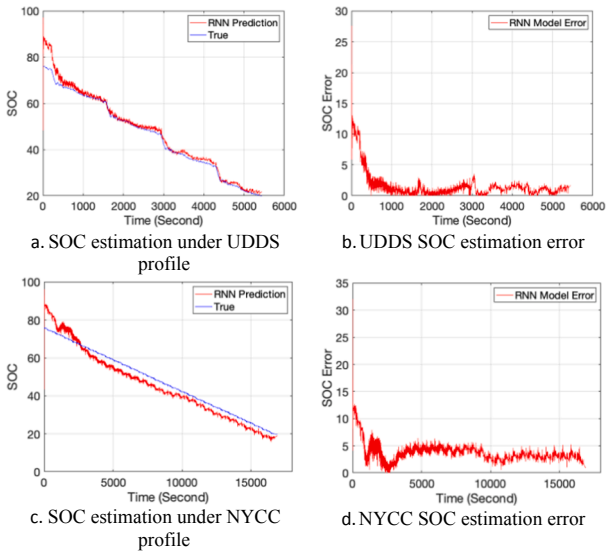

Fig. 7. Battery SOC prediction with partial UDDS (a and b), and NYCC (c and d) profiles with 76% initial true SOC using the trained TD-RNN from UDDS-NYCC profile.

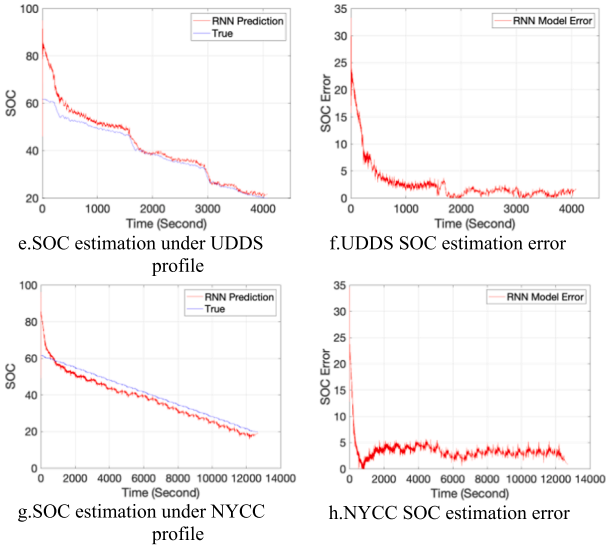

Fig. 8. Battery SOC prediction with partial UDDS (a and b), and NYCC (c and d) profiles with 61% initial true SOC using the trained TD-RNN from UDDS-NYCC profile.

performance of the TD-RNN on test conditions simply based on its training results. This phenomenon may apply to other neural network models, which influences the confidence of using them in practice. This study, through examining each neuron's output, discovers possible root causes for unstable performances of the TD-RNN. We call these abnormal neurons as 'overexcited' neurons, which might be the root cause for poor performance of the neural network under various operating conditions.

When running such training and testing process repeatedly for ten times, poor performances of the SOC estimation are all accompanied by these 'overexcited' neurons. Another example with 'overexcited' neurons is shown in Fig. 10a. Although the trained SOC matches the true SOC very well, the SOC estimation accuracy of the TD-RNN is relatively poor under two testing conditions as shown in Fig. 10c-f. On the other hand, accurate SOC estimation for testing conditions can be obtained when the neuron output is stable during the training stage as shown in

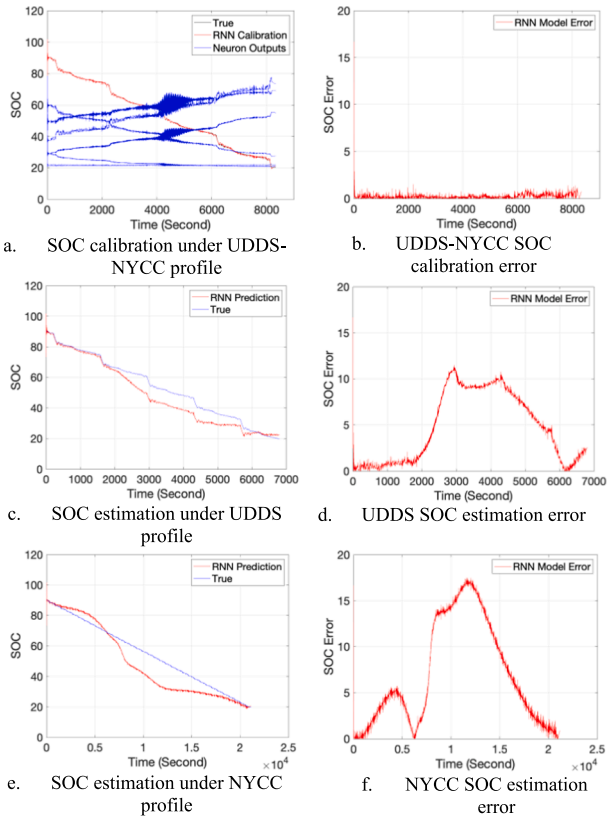

Fig. 9. TD-RNN with overexcited neurons using five time-delay steps and seven hidden neurons for battery SOC calibration and prediction under UDDS-NYCC (a and b), UDDS (c and d), and NYCC (e and f) profiles.

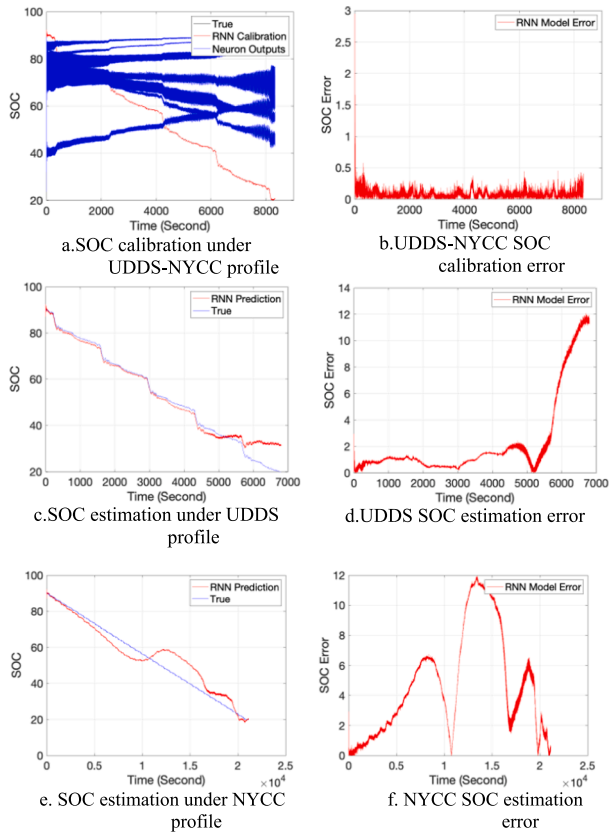

Fig. 10. TD-RNN with overexcited neurons and another local optimum using five time-delay steps and seven hidden neurons for battery SOC calibration and prediction under UDDS-NYCC (a and b), UDDS (c and d), and NYCC (e and f) profiles.

Fig. 6a.

5. Identification of overexcited neurons

Instead of finding 'overexcited' neurons through qualitative analysis, this section presents a way to quantitatively identify them through time–frequency analysis. 'Overexcited' neurons should contain relatively high power spectrum value (measured in dB) for non-zero frequencies at a certain period of time. For example, by conducting time–frequency analysis for neuron outputs in Fig. 9a, such a feature can be easily identified for each neuron as shown in Fig. 11. Among them, neuron 5, 6, and 7 are severer than others with higher power spectrum at about 350 mHz frequency between 1 and 1.5 h. Other neurons are also not healthy, although the power spectrum value is not as high as compared to these three neurons. As a comparison for neuron outputs shown in Fig. 6a where the TD-RNN shows exceptional performance for estimating the battery SOC, time–frequency analysis results are presented in Fig. 12. None of the neuron output shows high power spectrum value for frequency range above 50 mHz.

6. Discussion

6.1. Robustness of the TD-RNN for 'unseen' data sets

A good modeling technique, which can truly capture the real physics of the system, should not solely rely on abundant training data. Otherwise, its performance on new 'unseen' data sets may be unreliable. Considering actual discharge current profiles for lithium ion batteries, infinite amount of operating conditions is available. A common industry practice is to employ as much representative data as possible during the training, and provide 'warning' information for any 'unseen' data sets. Nevertheless, it is labor intensive and difficult to truly classify all

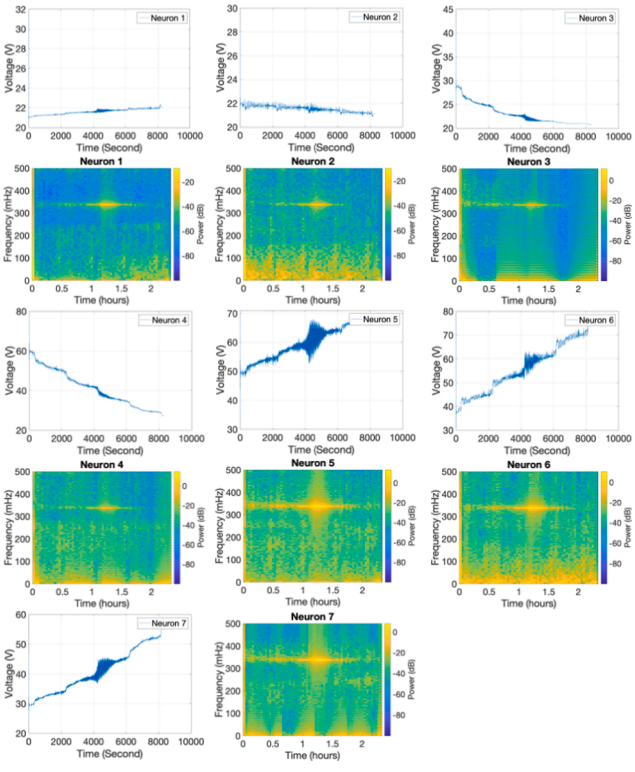

Fig. 11. Time frequency analysis for neuron outputs presented in Fig. 9a where the TD-RNN shows poor performance for battery SOC estimation.

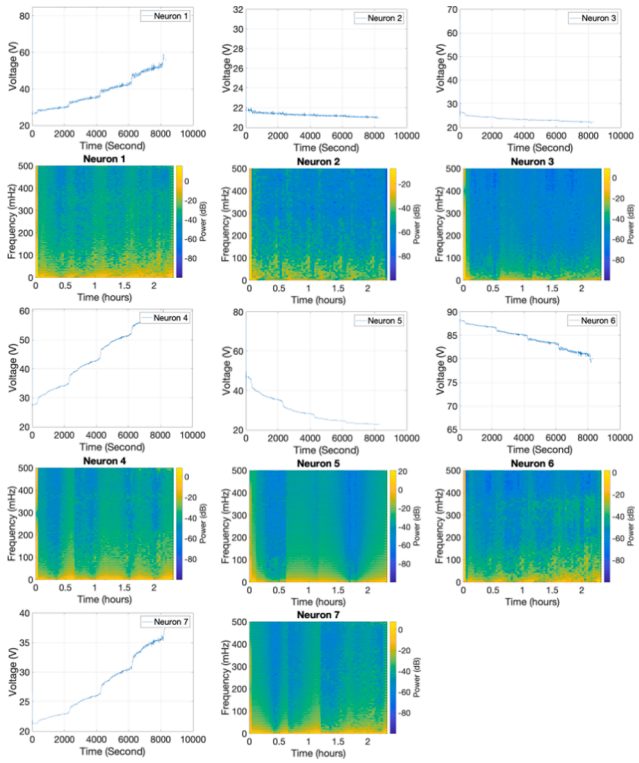

Fig. 12. Time frequency analysis for neuron outputs presented in Fig. 6a where the TD-RNN shows exceptional performance for battery SOC estimation.

'unseen' data sets for time series current and voltage profiles. As such, a good modeling technique should be able to tolerate some 'unseen' data sets. To further demonstrate the usefulness of 'overexcited' neurons for determining appropriate neural network structure for 'unseen' data sets, Fig. 13 shows the results of employing an inappropriate network structure for 'unseen' data sets. In particular, one time-delay step was employed for the TD-RNN but with twenty hidden neurons, in which 481 network parameters need to be determined. To create 'unseen' data sets for testing, the NYCC profile was used as the training and the other two profiles were employed for testing. There are continuous large discharge currents for the other two profiles resulting in abrupt SOC reductions, which are 'unseen' from the NYCC profile. It is clearly shown in Fig. 13a that many neuron outputs are 'overexcited' even though SOC calibration error is minimized as shown in Fig. 13b. Consequently, SOC estimation for the other two profiles contains large errors and unexplainable behaviors. Such unreliable and unpredictable performances of the neural network would prevent its wide adoption in reality. On the other hand, with proper network structure as identified before, in addition to stable neuron outputs as shown in Fig. 14a, the model is capable of providing reliable and accurate SOC estimation even for 'unseen' data sets as shown in Fig. 14c and d where the maximum SOC estimation error is less than 2.5%.

6.2. *Usage of 'overexcited' neurons*

With the capability of examining the 'overexcited' neurons, a proper TD-RNN structure for lithium ion battery states estimation can be more effectively determined. A recommended flowchart is shown in Fig. 15. Users can start with a set of TD-RNN structures (e.g., different number of time delay steps and hidden neurons). For each network structure, training can be repeated *M* times with random initial weights. Instead of simply selecting the training result with the best performance (e.g., the root mean squared error), we recommend to check 'overexcited' neurons in each training result for each network structure, and discard the training results if 'overexcited' neurons are identified. Finally, the training result with the best performance but without 'overexcited' neurons is considered as the most suitable TD-RNN structure.

6.3. *Comparison of the TD-RNN with the LSTM network and the extended Kalman filter (EKF)*

To demonstrate the effectiveness of the TD-RNN, the LSTM network and EKF were employed for comparison using the experimental data and the results are shown in Fig. 16. For the TD-RNN and LSTM network, the UDDS-NYCC profile was used as training data sets, and SOC under the other two profiles (i.e., UDDS and NYCC) was directly predicted. Same as the TD-RNN, the LSTM network only takes voltage and current as two input time series data for SOC prediction. Other network specifications include a layer of 500 LSTM hidden units, followed by a dropout layer with 30% dropout probability, followed by another layer with 50 fully connected hidden units, and followed by another dropout layer with

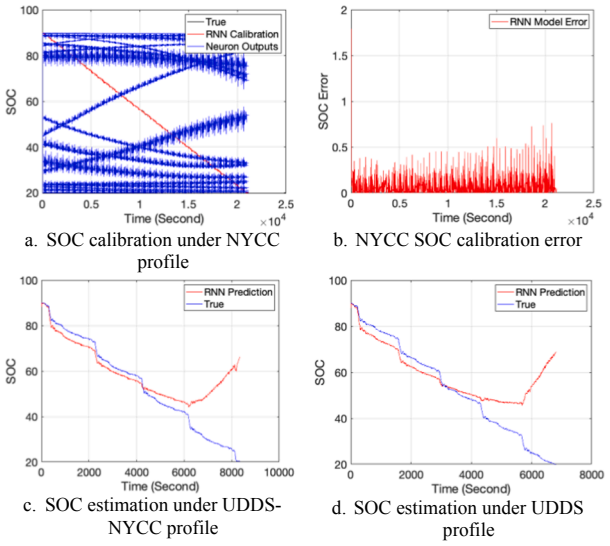

a. SOC calibration under NYCC profile
b. NYCC SOC calibration error
c. SOC estimation under UDDS-NYCC profile
d. SOC estimation under UDDS profile

Fig. 13. TD-RNN with overexcited neurons using one time-delay step and twenty hidden neurons for battery SOC calibration and prediction under NYCC (a and b), UDDS-NYCC (c), and UDDS (d) profiles.

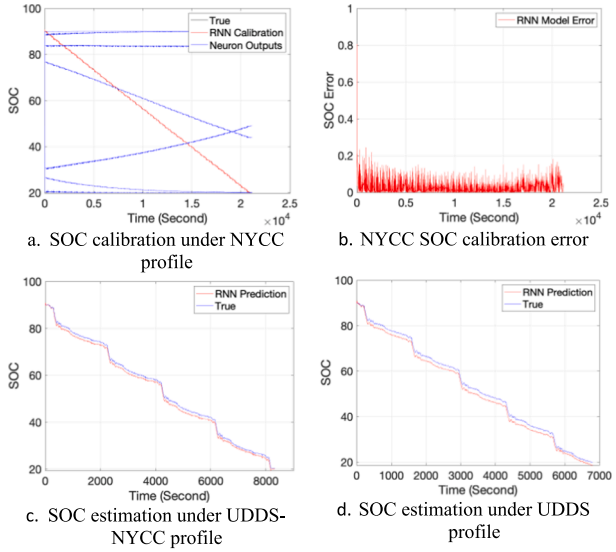

a. SOC calibration under NYCC profile
b. NYCC SOC calibration error
c. SOC estimation under UDDS-NYCC profile
d. SOC estimation under UDDS profile

Fig. 14. TD-RNN without overexcited neurons using five time-delay steps and seven hidden neurons for battery SOC calibration and prediction under NYCC (a and b), UDDS-NYCC (c), and UDDS (d) profiles.

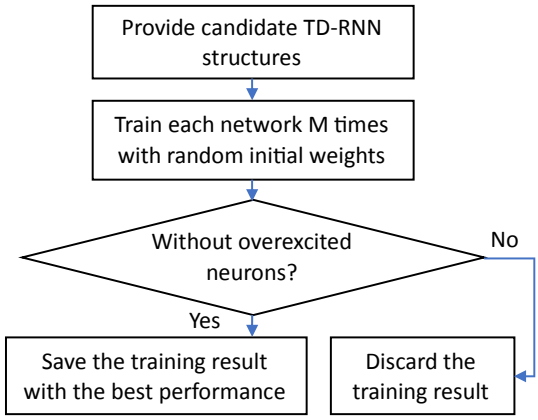

Fig. 15. Flowchart for selecting the best TD-RNN network through identification of the 'overexcited' neurons.

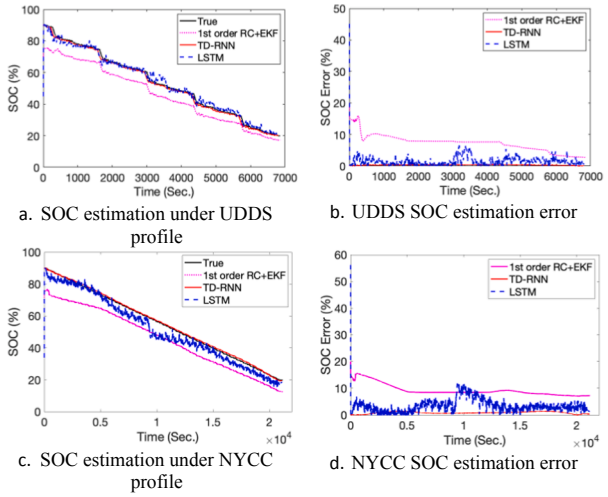

Fig. 16. Comparison of the TD-RNN with the LSTM network and EKF for battery SOC estimation under UDDS (a and b) and NYCC (c and d) profiles.

30% dropout probability to prevent overfitting. Trial and error process were taken in addition to referring to an existing work in reference [14] to obtain the results from the LSTM with reasonably good accuracy. The results from the EKF were obtained from authors' previous study based on the first order RC model with an initial guess of SOC at 70% [16]. Traditional feedforward neural networks (FNNs) were not considered for comparison because they generally do not outperform the LSTM based on the study in literature. In addition, extra features (e.g., average current and average voltage over a given time steps) need to be manually selected in FNNs to increase the SOC prediction accuracy.

Insightful findings are summarized as follows in the comparison study. Firstly, the TD-RNN shows consistent exceptional performances when choosing the results without 'overexcited' neurons. Secondly, the LSTM shows good accuracy especially compared to the results from the EKF. The SOC mean absolute error was calculated as 1.48% and 3.47% for UDDS and NYCC profile, respectively. It is worth noting that the sudden SOC drop in the NYCC profile as shown in Fig. 16c is the pattern exhibited in the training profile and is learned by the LSTM. Such a phenomenon is consistently observed even after changing the LSTM network configuration. Thirdly, as revealed in authors' previous work with appropriate convergence study of the EKF [16], the relatively large SOC estimation error from the first order RC model with the EKF is mainly because of the modeling error of the first order RC model combining with a fairly flat OCV-SOC curve for this Valence 26,250 lithium ion magnesium phosphate ($LiFeMgPO_4$) battery.

It is worth noting that more accurate SOC estimation with a smaller mean absolute error was reported in [14] using the LSTM network, e.g., 0.573% at one of the best validation configurations with proper training settings. There are two important differences between the two studies. The first difference is the battery type, i.e., $LiFeMgPO_4$ in this study vs. $LiNiCoAlO_2$ in [14]. Different battery characteristics could make the same algorithm to have different accuracy performances. The second major difference is the training and validation data sets selection. In this study, only one profile (i.e., UDDS-NYCC) was used as training and the other two (i.e., UDDS and NYCC) were used for validation. In the reference study [14], ten loading profiles were created from a mixture of four drive cycles. Among ten loading profiles, eight or nine profiles were used for training and the rest for validation. It is expected that the validation data sets may not be too much different compared to the training data sets. Considering these factors, the accuracy achieved for the LSTM network in this study is comparable to other reported results such as in [14,15].

7. Conclusion and future work

This paper proposed the TD-RNN for lithium ion battery SOC estimation. The proposed network structure can accurately characterize dependency of battery SOC as a time series function of battery current and terminal voltage. Although the studied battery ($LiFeMgPO_4$) possesses a flat OCV-SOC curve which imposes great challenges for traditional SOC estimation methods, the TD-RNN can achieve less than 1% SOC estimation accuracy with proper training of the network. Such an accuracy improvement can be considered as exceptional compared to previous study for the same battery using a bias learning method combined with an equivalent circuit model. More importantly, this paper further analyzed the poor performance of the TD-RNN, and proposed the concept of 'overexcited' neurons as potential root cause for unexpected overfitting or poor performance of the neural network. This assumption was validated through repeatedly training of the TD-RNN with random initial weights. The network without 'overexcited' neurons can estimate SOC accurately, whereas the network with 'overexcited' neurons usually show unexpected results under testing conditions. A good TD-RNN structure can thus be more effectively determined through examining the 'overexcited' neurons in addition to existing approaches. Comparison with the LSTM network reveals that the TD-RNN is more suitable for battery SOC estimation in addition to the fact that battery SOC should physically be determined by its most recent current and terminal voltage history.

Future work is to extend the TD-RNN for battery SOC and state of health (SOH) estimation. Similar to any data-driven methods, battery aging data will be used to train the TD-RNN. Other than using only current and voltage time series data as input features, battery SOH should also be incorporated as an input feature to model the coupling property between battery SOC and SOH. Effectiveness of the battery SOC and SOH estimation in practice should also consider other factors such as temperature and measurement noises.

CRediT authorship contribution statement

Zhimin Xi: Methodology, Software, Validation, Formal analysis, Investigation, Resources, Writing – original draft, Funding acquisition. **Rui Wang:** Methodology, Formal analysis, Investigation. **Yuhong Fu:** Software, Validation, Formal analysis, Investigation. **Chris Mi:** Software, Validation, Resources, Writing – review & editing, Funding acquisition.

Declaration of Competing Interest

The authors declare that they have no known competing financial interests or personal relationships that could have appeared to influence the work reported in this paper.

References

[1] Reimers JN, Dahn JR. Electrochemical and in situ x-ray diffraction studies of lithium intercalation in LixCoO2. J Electrochem Soc 1992;139(8):2091–7.
[2] Srinivasan V, Newman J. Discharge model for the lithium iron-phosphate electrode. J Electrochem Soc 2004;151(10):A1517–29.
[3] Gu WB, Wang CY. Thermal-electrochemical modeling of battery systems. J Electrochem Soc 2000;147(8):2910–22.
[4] Santhanagopalan S, White RE. Online estimation of the state of charge of a lithium ion cell. J Power Sources 2006;161(2):1346–55.
[5] Chaturvedi NA, Klein R, Christensen J, Ahmed J, Kojic A. Algorithms for Advanced Battery-Management Systems: Modeling, estimation, and control challenges for lithium-ion batteries. IEEE Control Syst 2010;30(3):49–68.
[6] Hu X, Li S, Peng H. A comparative study of equivalent circuit models for Li-ion batteries. J Power Sources 2012;198:359–67.
[7] Fotouhi A, Auger DJ, Propp K, Longo S, Wild M. A review on electric vehicle battery modelling: From Lithium-ion toward Lithium-Sulphur. Renew Sustain Energy Rev 2016;56:1008–21.
[8] Chiang, Y.-., Sean, W.-. & Ke, J.-. 2011, Online estimation of internal resistance and open-circuit voltage of lithium-ion batteries in electric vehicles, Journal of Power Sources, vol. 196, no. 8, pp. 3921-3932.
[9] Dai H, Wei X, Sun Z, Wang J, Gu W. Online cell SOC estimation of Li-ion battery packs using a dual time-scale Kalman filtering for EV applications. Appl Energy 2012;95:227–37.
[10] Nejad S, Gladwin DT, Stone DA. A systematic review of lumped-parameter equivalent circuit models for real-time estimation of lithium-ion battery states. J Power Sources 2016;316:183–96.
[11] Kang L, Zhao X, Ma J. A new neural network model for the state-of-charge estimation in the battery degradation process. Appl Energy 2014;121:20–7.
[12] Chaoui H, Ibe-Ekeocha CC, Gualous H. Aging prediction and state of charge estimation of a LiFePO4 battery using input time-delayed neural networks. Electr Power Syst Res 2017;146:189–97.
[13] Xia B, Cui D, Sun Z, Lao Z, Zhang R, Wang W, et al. State of charge estimation of lithium-ion batteries using optimized Levenberg-Marquardt wavelet neural network. Energy 2018;153:694–705.
[14] Chemali E, Kollmeyer PJ, Preindl M, Ahmed R, Emadi A. Long Short-Term Memory Networks for Accurate State-of-Charge Estimation of Li-ion Batteries. IEEE Trans Ind Electron 2018;65(8):6730–9.
[15] Yang, F., Song, X., Xu, F. & Tsui, K.-. 2019, State-of-Charge Estimation of Lithium-Ion Batteries via Long Short-Term Memory Network, IEEE Access, vol. 7, pp. 53792-53799.
[16] Xi Z, Dahmardeh M, Xia B, Fu Y, Mi C. Learning of Battery Model Bias for Effective State of Charge Estimation of Lithium-Ion Batteries. IEEE Trans Veh Technol 2019;68(9):8613–28.
[17] Hong, J., Wang, Z., Chen, W., Wang, L.-. & Qu, C. 2020, Online joint-prediction of multi-forward-step battery SOC using LSTM neural networks and multiple linear regression for real-world electric vehicles, Journal of Energy Storage, vol. 30.
[18] Lee CW, Hong Y, Hayrapetyan M, Yang XG, Xi Z. Derivation and tuning of a solvable and compact differential–algebraic equations model for LiFePO4–graphite Li–ion batteries. J Appl Electrochem 2018;48(3):365–77.
[19] Plett GL. Extended Kalman filtering for battery management systems of LiPB-based HEV battery packs - Part 3. State and parameter estimation. J Power Sources 2004;134(2):277–92.
[20] Miao Q, Xie L, Cui H, Liang W, Pecht M. Remaining useful life prediction of lithium-ion battery with unscented particle filter technique. Microelectron Reliab 2013;53(6):805–10.
[21] Dahmardeh M, Xi Z. "State-of-charge uncertainty of lithium-ion battery packs considering the cell-to-cell variability", ASCE-ASME Journal of Risk and Uncertainty in Engineering Systems, Part B. Mechanical Engineering 2019;5:no. 2.
[22] Srivastava N, Hinton G, Krizhevsky A, Sutskever I, Salakhutdinov R. Dropout: A simple way to prevent neural networks from overfitting. Journal of Machine Learning Research 2014;15:1929–58.